

Supporting information

Additional methods and instrumentation.....	2
Scheme S1. Synthetic route of Ligand H ₄ L.....	4
Scheme S2. Schematic diagram of the synthesis of MOF 1.....	4
Scheme S3. The view of the structural skeleton for three antibiotics used in this work.....	5
Table S1. Structures comparison of MOFs synthesized by similar main ligands and N-donor ligands.....	6
Table S2. Crystal data and structure refinement parameters of MOF 1.....	12
Table S3. Partial bond lengths (Å) and bond angles (°) of MOF 1.....	14
Table S4. The view of the degradation effiency of OXY in different condtion.....	15
Figure S1. A 2D topological view of MOF 1.....	16
Figure S2. FT-IR MOF 1.....	16
Figure S3. PXRD of MOF 1.....	17
Figure S4. TGA of MOF 1.....	17
Figure S5. Solid-state optical diffuse-reflection spectra of 1 derived from diffuse reflectance data at ambient temperature.....	18
Figure S6. The recycle experiments revealed an overall drop of 5% in the photocatalytic performance of 1.....	18
Figure S7. SEM photos before and after photocatalysis reaction for MOF 1.....	19
References.....	20

Additional methods and instrumentation

S1. X-ray crystallography

The single crystal data for **1** were collected by a Bruker D8 VENTURE Metaljet PHOTON II single crystal diffractometer. The crystal was kept at 193.0 K during data collection. The crystal structure was elucidated by the direct method of the SHELXT program. All non-hydrogen atomic coordinate data were obtained by Fourier synthesis, and anisotropic thermal parameters were refined. The coordinates of the hydrogen atoms were calculated theoretically and refined isotropically. Table S2 is the crystal data and structure refinement parameters of MOF **1**, and Table S3 presents the pertinent bond lengths (Å) and bond angles (°) of MOF **1**.

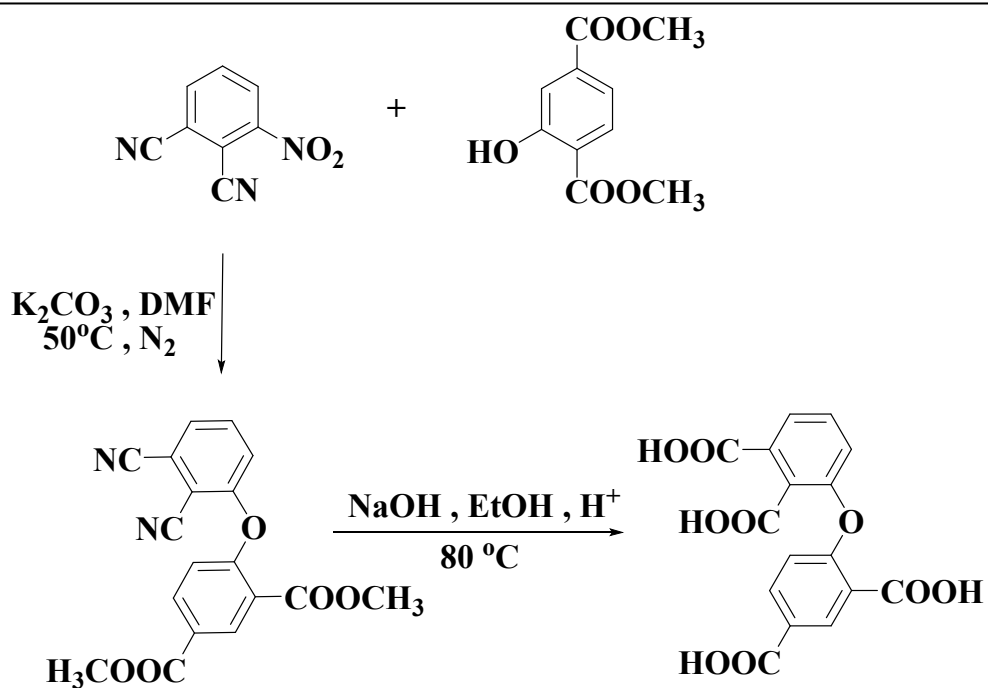
S2. Synthesis of ligand

Ligand synthesis according to references.¹⁻³ To a solution of methyl 2-hydroxyterephthalate (1 mmol) in DMF (20 mL) was added K₂CO₃ (0.28 g, 2.029 mmol), followed by stirring for 0.5 hours. Then 3-nitrophthalonitrile (0.73 g, 1 mmol) was added to the mixed solution, and the mixture was heated to 50 °C under nitrogen and stirred for 24 hours. The reaction mixture was then cooled to room temperature, and the K₂CO₃ was removed by filtration. The filtrate was poured into 50 mL of ice water at 2°C, and a large amount of precipitate was rapidly formed. The precipitate was filtered, dried, and mixed with ethanol (1 mL) and sodium hydroxide (20 mL, 4M) and heated under reflux until the hydrolysis is complete. The reaction mixture was cooled to room temperature, undissolved substances were removed by filtration, hydrochloric acid solution (6M) was added to the filtrate, and when pH was adjusted to 2, precipitation occurred, and after standing, the resulting solid was rinsed with distilled water and dried to obtain the target product (H₄L) 0.1009 g (yield 57.8%). IR (cm⁻¹, KBr): 3407(w), 3235(m), 2989(m), 2548(w), 1705(s), 1612(s), 1460(m), 1402(s), 1245 (s), 1126(m), 1074(m), 961(m), 766(s), 618(s). The synthetic route is shown in Fig. S1.

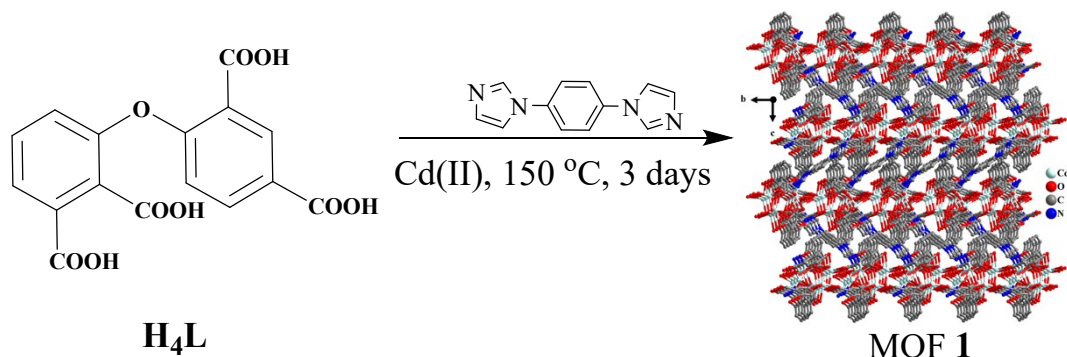
S3. Characterizations.

All the chemical reagents and drugs used in this study were purchased from

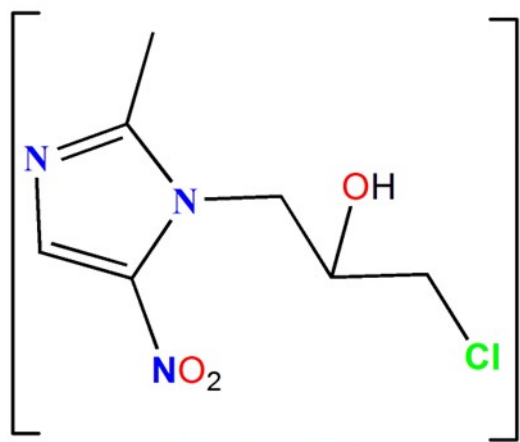
commercial sources and were used without further purification. The Fourier transform infrared (FT-IR) spectrum was recorded in the range of 4000-400 cm⁻¹ on a Bruker VERTEX 70 spectrometer using KBr pellets. Elemental analyses (C, H, and N) were carried out on a VxRio EL elemental analyzer. Powder X-ray diffraction (PXRD) patterns were collected in the 2θ=5-45° range on a Philips PW 1710-based diffractometer with GaKα radiation ($\lambda=0.154184$ nm) at room temperature, operated at 40 kV and 100 mA. Thermogravimetric analysis (TGA) was performed on a PerkinElmer TG-7 analyzer heated from room temperature to 800 °C under nitrogen at a heating rate of 10 °C /min. UV-Vis DRS spectra were recorded on a U-3900H Spectrophotometer.



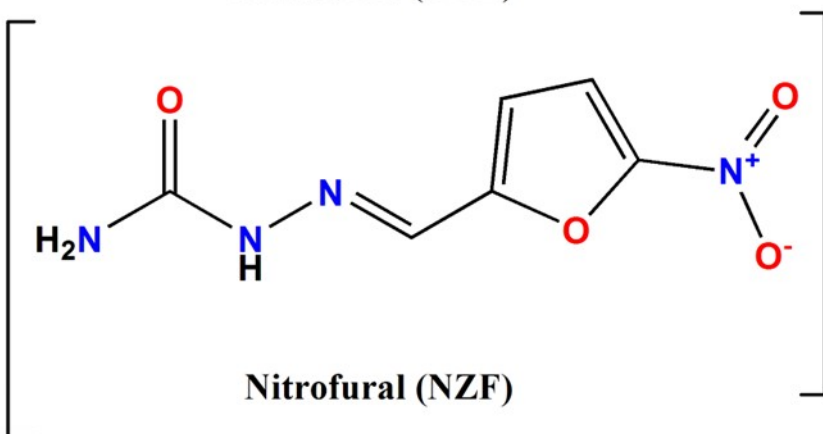
Scheme S1. Synthetic route of Ligand H₄L.



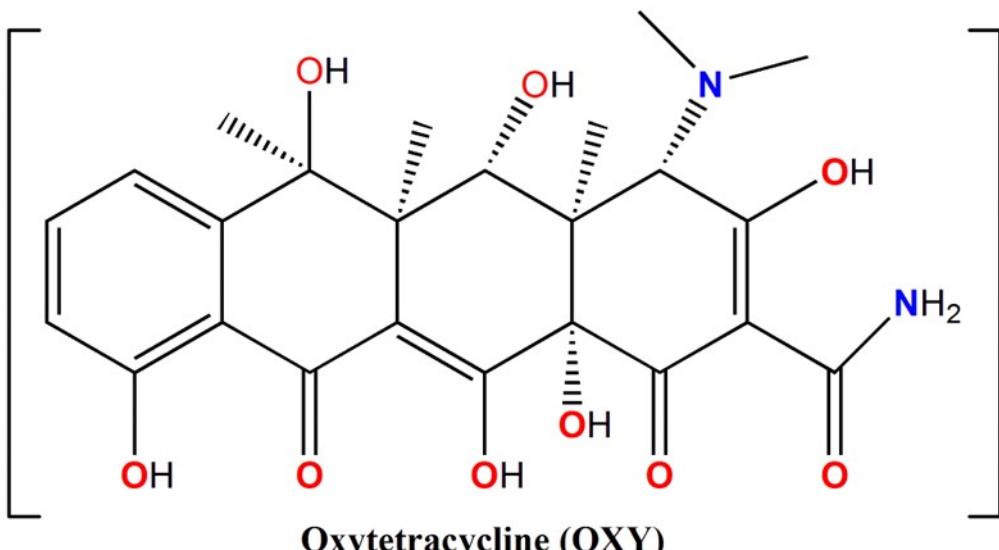
Scheme S2. Schematic diagram of the synthesis of MOF 1.



Ornidazole (ODZ)



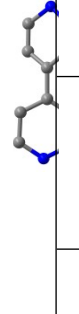
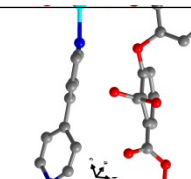
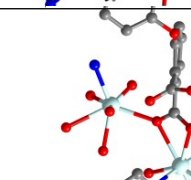
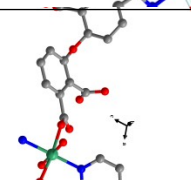
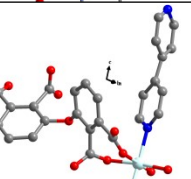
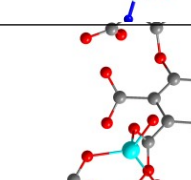
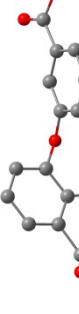
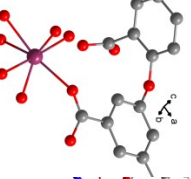
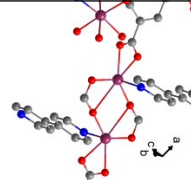
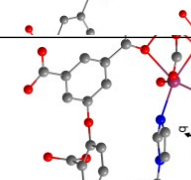
Nitrofural (NZF)

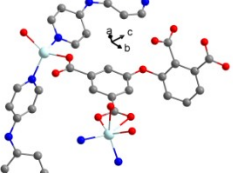
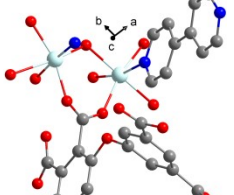
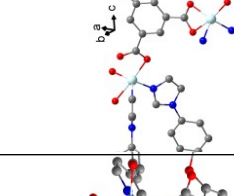
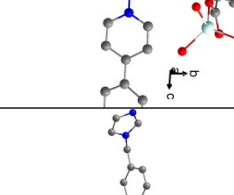
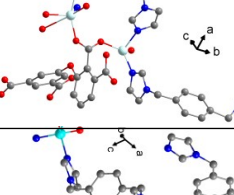
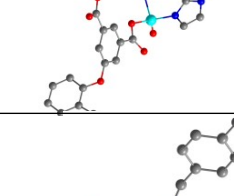
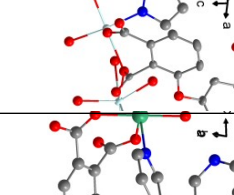
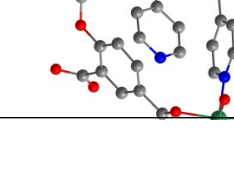
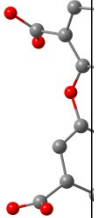
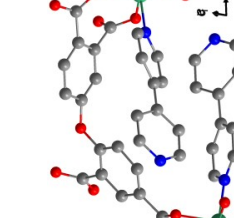
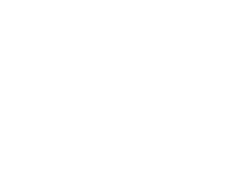


Oxytetracycline (OXY)

Scheme S3. The view of the structural skeleton for three antibiotics used in this work.

Table S1. Structures comparison of MOFs synthesized by similar main ligands and N-donor ligands.

Main ligand	N-donor ligand	Meta 1 ion	Cell diagram	Coordination number	Topology point	Dimension	Property	Ref.
		Zn		6	/	2-D	Fluorescent Emission	7
		Cd		7	/	2-D		
		Ni		6	/	3-D	Magnetic Property	8
		Co		6	/	3-D		
		Zn		4 and 6	/	1-D	Magnetic Property	9
		/		7	/	0-D	/	10
				6	$(4.5^2)_2$ $(4^2.6^8.8^3.9^2)$ $(5^2.8.9^2.10)$	3-D	Magnetic Property	11
		Mn		6	$(6^3.8^3)_2(8^5.10)$	3-D		

				6	$(4^2.6^4)$	3-D		
	Co			6	$(4^3)_2(4^6.6^{18}.8^4)$	3-D		
				5	$\{6^4.8^2\}$	3-D		
				5 and 6	$(6^3.8^3)(6^3)(8^3)$	3-D		
				4 and 6	$(4.5.6.8^3)$ $(4^2.5^3.6)$ $(4^3.5^3.6^2.7^2)$	3-D	Magnetic Property	12
				4 and 5	$(4^3)_2(4^6.6^{18}.8^4)$	3-D		
				5 and 6	$(4^3)_2(4^6.6^{18}.8^4)$	3-D		
	Ni			6	$\{4.6^4.8\}_2\{4^2.6^4.8^9\}\{6^2.8\}_2$	3-D	Fluorescent Emission	13

				6	/	0-D	Photocatalytic Degradation	14
	Co			6	/	0-D		
	Mn			6	/	1-D		
	/	Co		6	(6 ⁵ .8)	3-D	Magnetic Property	15
		Co		6	(4 ² .6 ³ .8)	3-D		
		Co		6	(4.6 ⁴ .8)(4.6 ⁵)	3-D		
		Zn		4 and 6	(4 ² .6 ³ .8)	3-D		
		Zn		4 and 5	(4 ⁴ .6 ⁶)	3-D		
				5 and 6	/	2-D	Fluorescent Emission	16

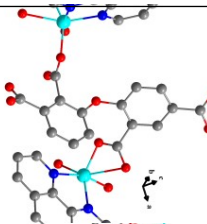
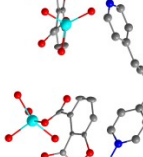
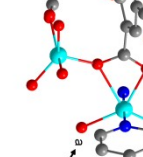
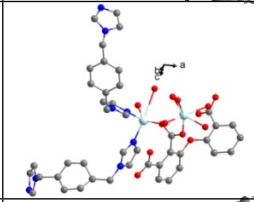
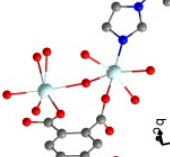
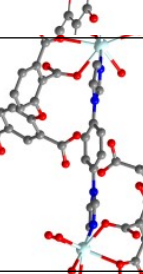
				6	$\{4.6^4.8\}_2\{4^2.6^2.8^2\}$	3-D		
	Cd			4 and 5	$\{4^3\}_2\{4^6.6^{18}.8^4\}$	3-D	Fluorescent Emission	17
				5 and 6	$\{3^2.4^2.5^2\}_2\{3^4.4^2.6^{19}.7^2.8\}\{3^4.4^4.5^4.6^2.8\}$	3-D	Fluorescent Emission	
		Co		5 and 6	$\{4^3.6^3\}\{4^3.6^9.8^3\}$	3-D	Magnetic Property	18
	Cd			6	$\{4^3\}_2\{4^6.6^{14}.8^8\}$	3-D	Fluorescent Emission	
				6 and 7	$\{3^6.4^{18}.5^3.6\}$	3-D	Photocatalytic Degradation	This work

Table S2. Crystal data and structure refinement parameters of **1**.

MOF	1
Empirical formula	C ₄₄ H ₃₀ Cd ₄ N ₄ O ₂₂
Formula weight	1416.32
Temperature/K	193
Crystal system	monoclinic
Space group	Cc
<i>a</i> /Å	12.7703(8)
<i>b</i> /Å	16.1875(10)
<i>c</i> /Å	22.0193(14)
α /°	90
β /°	96.415(3)
γ /°	90
Volume/Å ³	4523.3(5)
<i>Z</i>	4
ρ_{calc} g/cm ³	2.08
μ /mm ⁻¹	10.671
<i>F</i> (000)	2760
Crystal size/mm ³	0.12 × 0.1 × 0.1
Radiation	GaKα ($\lambda = 1.34139$)
2θ range for data collection/°	7.702 to 120.646
Index ranges	-14 ≤ <i>h</i> ≤ 16, -19 ≤ <i>k</i> ≤ 20, -28 ≤ <i>l</i> ≤ 27
Reflections collected	29397
Independent reflections	9496 [R _{int} = 0.0526, R _{sigma} = 0.0557]
Data/restraints/parameters	9496/3/676
Goodness-of-fit on <i>F</i> ²	1.049
Final <i>R</i> indexes [<i>I</i> >=2σ (<i>I</i>)]	R ₁ = 0.0328, wR ₂ = 0.0694
Final <i>R</i> indexes [all data]	R ₁ = 0.0385, wR ₂ = 0.0717
Largest diff. peak/hole / e Å ⁻³	0.53/-0.96

Flack parameter	0.394(9)
$R_1 = \sum F_o - F_c / \sum F_o $.	
$wR_2 = [\sum w(F_o^2 - F_c^2)^2 / \sum w(F_o^2)^2]^{1/2}$, $w = [\sigma^2(F_o^2) + (0.0784P)^2 + 1.3233P]^{-1}$, where $P = (F_o^2 + 2F_c^2)/3$.	
GOF = $[\sum w(F_o^2 - F_c^2)^2 / (n_{\text{obs}} - n_{\text{param}})]^{1/2}$	

Table S3. Partial bond lengths (\AA) and bond angles ($^\circ$) of MOF 1.

Bond	Length/\AA	Bond	Length/\AA	Bond	Length/\AA
Cd2-O16#1	2.229(5)	Cd4-O3#3	2.562(5)	Cd1-O11#2	2.530(5)
Cd2-O17#1	2.511(5)	Cd4-O14	2.618(6)	Cd1-O6	2.498(5)
Cd2-O18	2.168(5)	Cd4-O22	2.369(6)	Cd1-O20	2.400(5)
Cd2-O4	2.262(5)	Cd4-O8	2.305(5)	Cd1-N4	2.210(7)
Cd2-O11#2	2.209(5)	Cd4-N1#4	2.228(6)	Cd3-O2#3	2.265(5)
Cd2-O12#2	2.639(6)	Cd1-O3	2.193(5)	Cd3-O7#5	2.316(5)
Cd4-O2#3	2.409(5)	Cd1-O19	2.309(5)	Cd3-O1#3	2.533(6)
Cd4-O13	2.230(5)	Cd1-O14#2	2.539(5)	Cd3-O6#5	2.380(5)
Bond	Angle/$^\circ$	Bond	Angle/$^\circ$	Bond	Angle/$^\circ$
O16#1-Cd2-O17#1	54.81(18)	O3#3-Cd4-O14	70.05(16)	O19-Cd1-O6	76.04(19)
O16#1-Cd2-O4	109.9(2)	O22-Cd4-O2#3	171.53(19)	O19-Cd1-O20	147.4(2)
O16#1Cd2-O12#2	92.88(19)	N1#4-Cd4-O2#3	95.7(2)	N4-Cd1-O19	87.5(2)
O17#1-Cd2-O12#2	76.74(19)	N1#4-Cd4-O13	173.9(2)	N4-Cd1-O14#2	81.6(2)
O18-Cd2-O16#1	96.7(2)	N1#4-Cd4-O3#3	82.4(2)	N4-Cd1-O11#2	90.3(2)
O18-Cd2-O17#1	149.2(2)	N1#4-Cd4-O14	120.4(2)	N4-Cd1-O6	110.0(2)
O1-Cd2-O4	106.0(2)	N1#4-Cd4-O22	78.8(2)	N4-Cd1-O20	89.4(2)
O18-Cd2-O11#2	113.4(2)	N1#4-Cd4-O8	96.5(2)	O2#3-Cd3-O7#5	89.92(19)
O18-Cd2-O12#2	95.5(2)	O3-Cd1-O19	108.87(19)	O2#3-Cd3-O1#3	54.64(18)
O2#3-Cd4-O3#3	71.18(16)	O3-Cd1-O14#2	77.46(18)	O2#3-Cd3-O6#5	140.67(18)
O2#3-Cd4-O14	121.34(17)	O3-Cd1-O11#2	80.21(18)	O7#5-Cd3-O1#3	76.6(2)
O13-Cd4-O2#3	88.39(19)	O3-Cd1-O6	87.30(18)	O7#5-Cd3-O6#5	55.75(18)
O13-Cd4-O3#3	94.72(17)	O3-Cd1-O20	83.7(2)	O10-Cd3-O2#3	91.8(2)
O13-Cd4-O14	53.58(17)	O3-Cd1-N4	159.0(2)	O10-Cd3-O7#5	95.1(2)
O13-Cd4-O22	97.6(2)	O19-Cd1-O14#2	144.80(19)	O10-Cd3-O1#3	144.79(19)
O13-Cd4-O8	88.4(2)	O19-Cd1-O11#2	79.45(19)	O10-Cd3-O6#5	108.3(2)

Symmetry codes: #1: -1/2+x,-1/2+y,+z; #2: -1+x,+y,+z; #3: 1+x,+y,+z; #4: 1+x,1-y,-1/2+z; #5:

1/2+x,-1/2+y,+z; #6: 1/2+x,1/2+y,+z; #7: -1/2+x,1/2+y,+z; #8: -1+x,1-y,1/2+z.

Table S4. The view of the degradation efficiency of OXY in different condition.

OXY concentration	70 mg/L	80 mg/L	90 mg/L
	75.8 %	77.0 %	76.2 %
Dosage 1	20 mg	25 mg	30 mg
	76.1 %	77.0 %	73.7 %
pH	pH=5	pH=6	pH=7
	34.2 %	77.0 %	70.4 %

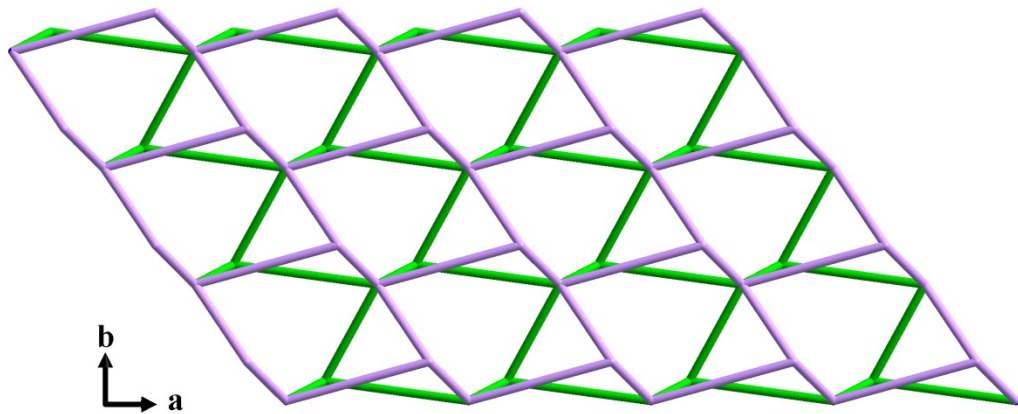


Figure S1. A 2D topological view of **1**.

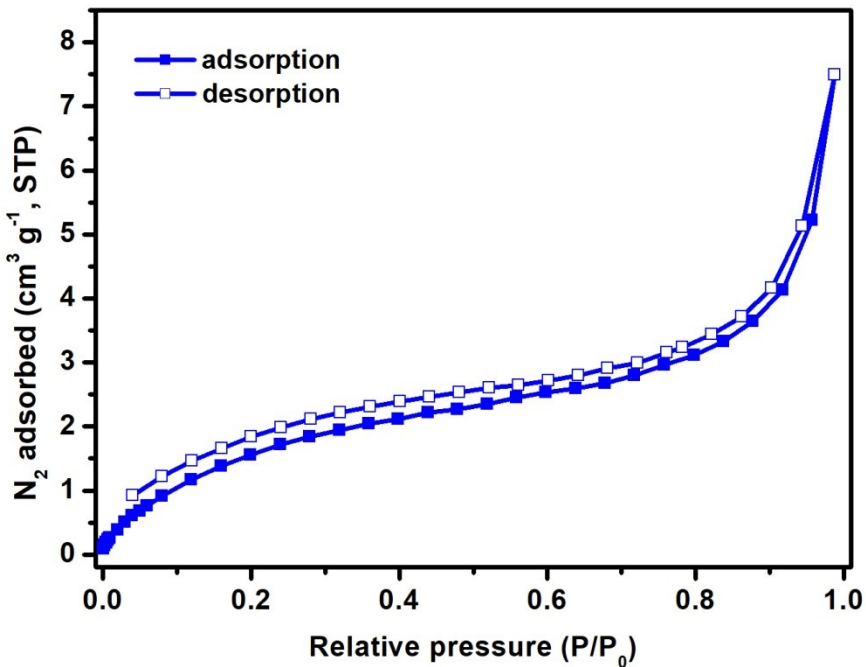


Figure S2 view of the BET of **1**.

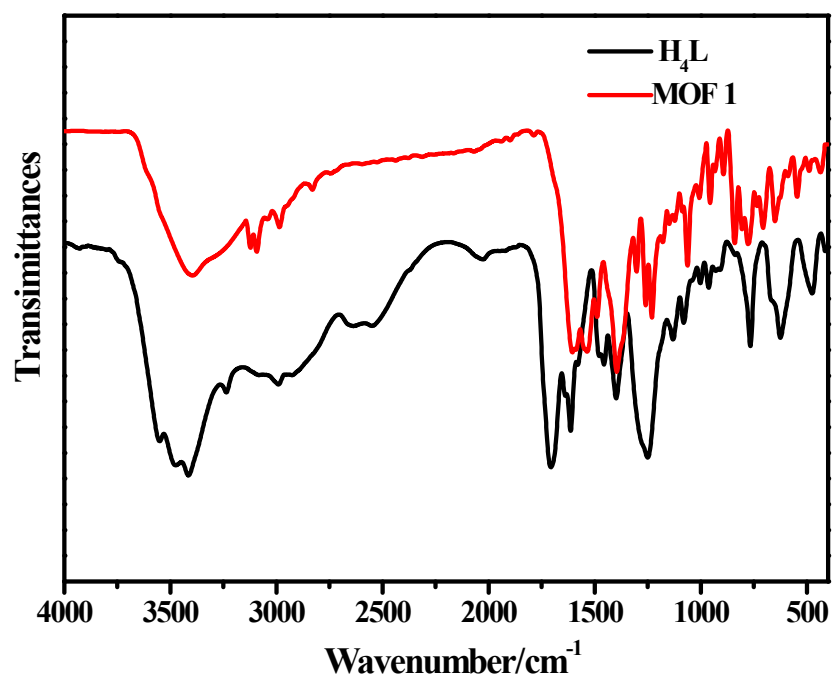


Figure S3. FT-IR of **1**.

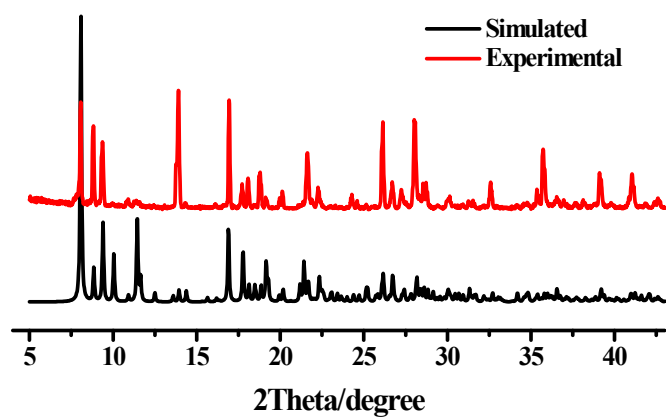


Figure S4. PXRD of **1**.

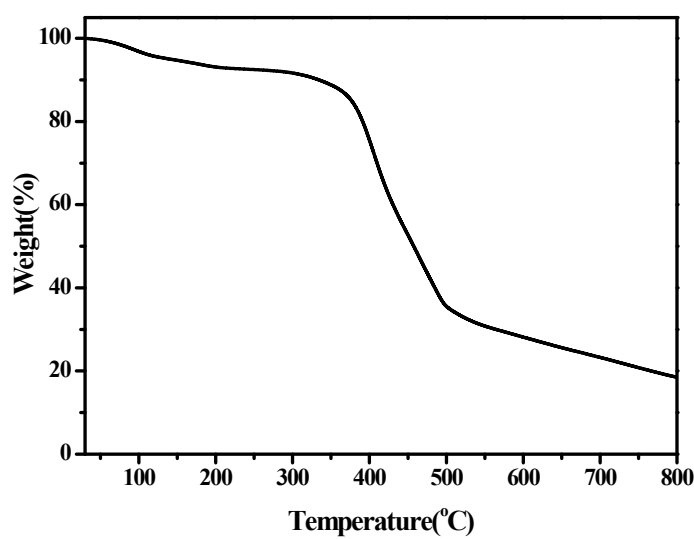


Figure S5. TAG of **1**.

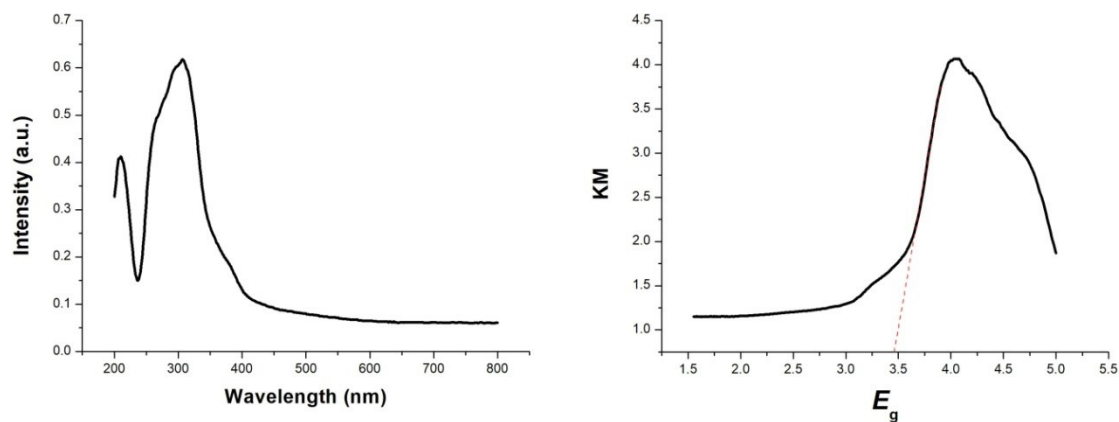


Figure S6. Solid-state optical diffuse-reflection spectra of **1** derived from diffuse reflectance data at ambient temperature.

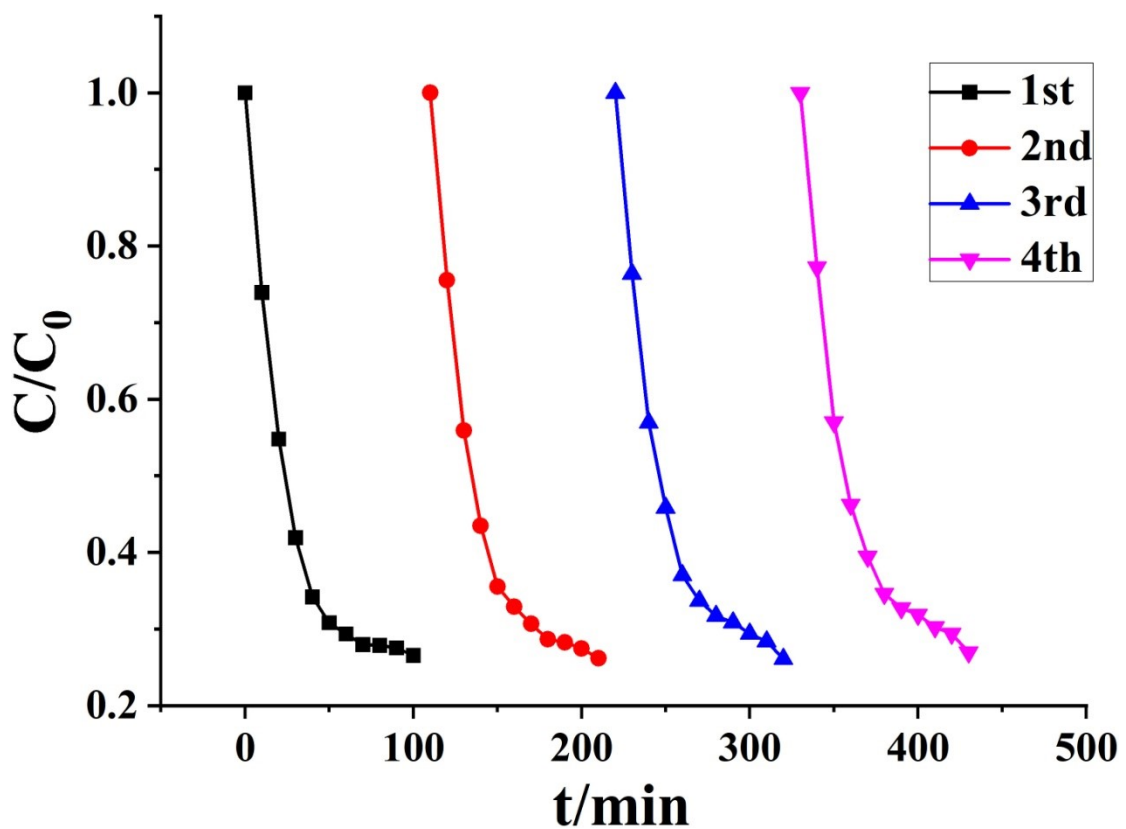


Figure S7. The recycle experiments revealed an overall drop of 5% in the photocatalytic performance of **1**.

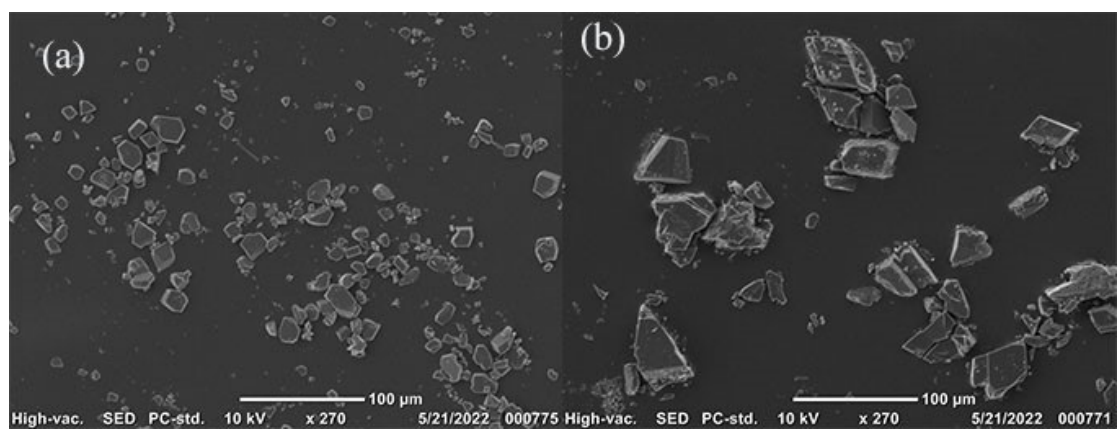


Figure S8. SEM photos before and after photocatalysis reaction for MOF **1**.

- [1] S. Zhang, F. Jiang, M. Wu, J. Ma, Y. Bu, M. Hong, Cryst. Growth Des., 2012, **12**, 1452-1463.
- [2] H. Wang, D. Zhang, D. Sun, Y. Chen, L. Zhang, L. Tian, and J. Jiang, Cryst. Growth Des., 2009, **9**, 5273-5282.
- [3] C. Si, D. Hu, Y. Fan, Y. Wu, X. Yao, Y. Yang, and J. Liu. Cryst. Growth Des., 2015, **15**, 2419-2432.
- [4] G. M. Sheldrick. Acta Crystallogr A Found Crystallogr, 2008, **64**, 112-122.
- [5] W. Silen, T. Machen and J. Forte. Am J Physiol, 1975, **229**, 721-730.
- [6] O. Dolomanov, L. Bourhis, R. Gildea, J. Howard and H. Puschmann. J Appl Crystallogr, 2009, **42**, 339-341.
- [7] S. Zang, Y. Su, Y. Li, Z. Ni and Q. Meng, Inorg. Chem., 2006, **45**, 174-180.
- [8] S. Zang, Y. Su, Y. Li, H. Zhu and Q. Meng, Inorg. Chem., 2006, **45**, 2972-2978.
- [9] S. Zang, Y. Su, J. Lin, Y. Li, S. Gao and Q. Meng, Inorganica Chim., 2009, **362**, 2440-2446.
- [10] L. Jing and L. Jing, Z. Kristallogr. - New Cryst. Struct., 2016, **231**, 771-773.
- [11] X. Li, G. Liu, L. Xin and L. Wang, J. Solid State Chem., 2017, **246**, 252-257.
- [12] Dong, C. Si, Y. Fan, D. Hu, X. Yao, Y. Yang and J. Liu, Cryst. Growth Des., 2016, **16**, 2062-2073.
- [13] C. Song, X. Li, W. Liu, Z. Cao, Y. Ren, Q. Zhou and L. Zhang, Synth. React. Inorg. Met.-Org., 2016, **46**, 1787-1791.
- [14] C. Wang, Y. Zhang, T. Zhu, X. Zhang, P. Wang and S. Gao, Polyhedron, 2015, **90**, 58-68.
- [15] Y. Peng, G. Li, J. Hua, Z. Shi and S. Feng, CrystEngComm, 2015, **17**, 3162-3170.
- [16] Y. Yu, J. Mol. Stuct., 2017, **1149**, 761-765.
- [17] P. Zhou, Z. Anorg. Allg. Chem., 2017, **643**, 325-329.
- [18] D. Xiong, Y. Li, Z. Shi, T. Qin, D. Li, P. Fu, Q. Yang, Y. Zhu and X. Dong, J. Mol. Stuct., 2022, **1254**, 132343.